Heidelberg University
Institute of Computer Science
Visual Computing Group (VCG)

Master-Arbeit

Global Illumination Techniques for Tensor Field Visualization

Sebastian Bek	
Matrikelnummer:	3481802
Betreuer:	Sebastian Bek
Datum der Abgabe:	07.07.2019

dt.: Ich versichere, dass ich diese Master-Arbeit selbstständig verfasst und nur die angegebenen Quellen und Hilfsmittel verwendet habe und die Grundsätze und Empfehlungen "Verantwortung in der Wissenschaft" der Universität Heidelberg beachtet wurden.

eng.: I hereby declare/assure, that I drafted this thesis independently and only used the sources and materials labeled as references and that the conventions/principles and recommendations "Verantwortung in der Wissenschaft" of the Heidelberg University have been regarded/observed.

Abgabedatum / Due Date: 07.07.2019

Zusammenfassung

Tensorfelder werden meistens in Verbindung mit mechanischen Spanunngsverteilungen in 2D/3D-Gittern gebracht (vgl. Cauchy-Stress Tensor), haben aber auch andere praktische Bedeutungen in der Physik. Mithilfe von globalen Beleuchtungsmodellen/-techniken wird eine neue Methode entwickelt, um Tensorfelder zu visualisieren. Als Grundlage leiten wir ein einfaches Lichtausbreitungsschema für kartesische Gitter ab, dass die Prinzipien der Ausbreitungsdämpfung und Energieerhaltung beachtet und Lichtverteilung/en für gegebene Lichtquellenrichtung/en und -positionen bis zur Konvergenz approximieren kann. Als unterliegendes Modell werden die Transmissionsprofile innerhalb diesem Gitter als Kristallfiberstruktur angenommen (vgl. Edelsteine: Katzenaugeneffekt beim Tigerauge). Die folgende Aufgabe ist es, anisotrope Fiberstrukturen mit der Orientierung und den Anisotropiemaßen des unterliegenden Tensorfelds zu modellieren. Dafür erstellen wir per Hauptachsentransformation (PCA) ein Eigensystem für jede Zelle des Tensorfelds und modellieren eine zugehörige Ellipsengleichung als (Transfer-/Wichtungs-) Transmissionsprofil. Wir messen Impulsantworten des Tensorfelds mit Delta-Pulsen an jeder Position und in jede Richtung um eine uniform gesamplete Map der globalen Lichtverteilungen zu erhalten. Diese Map wird als ein globales Energieflussfeld betrachtet. Wir lassen uns von der Technik FTLE aus dem Bereich Particle Tracing der Vector Field Visualization inspirieren, indem wir den Gradient des Flussfelds der resultierenden Lichtverteilungen analysieren und visualisieren. Ähnlich wie FTLE in Vektorfeldern Gräte/Kämme/LCS detektiert, erfasst unsere Methode dieselben Strukturen, anziehende/abstoßende/sattelnde Tensorfeldlinien die häufig Schlüsselstrukturen in der Natur repräsentieren, in Tensorfeldern. Wir führen diese Größe als Global Illumination Gradient ein, der einen FTLE-verwandten Ansatz darstellt, um LCS in Tensorfeldern durch die Analyse des globalen, durch einen Imprint (Gravur in kristallinen Fiberstrukturen) gerichteten Lichtflusses, zu visualisieren. Außerdem führen wir Deformation Ellpsoid Glyphen ein, die zusätzlich zur Darstellung der anisotropen Topologie die Richtung(Zug-/Druck) der Spannung durch Pfeile nach innen/außen darstellen. Das Verfahren wird in einer extensiven Evaluationsphase auf Plausibilität und Vergleichbarkeit geprüft.

Abstract

Tensor Fields, are most commonly associated with stress distributions (cnf. Cauchy-Stress Tensor) in 2D/3D grids, but also have some other meanings in practice in physics. By means of global illumination techniques we develop a new method to visualize tensor fields. As a basis, we derive a simple light propagation scheme for Cartesian grids, which satisfies propagation attenuation and energy-conservation principles and is able to approximate light distributions for given light source position(s) and direction(s) until convergence. The transmission profiles within this grid are considered as crystal fiber structures as an underlying physical model (eg. gemstones: tiger's eye's cat's eye effect). The consequent task is to model anisotropic fibre structures with the orientation and anisotropy measures of the underlying tensor field in the grid. For this, we derive an eigenbasis by PCA (principal component analysis) for every cell of the tensor field and form an ellipsoid equation as transmission (transfer/weighting) function for the transmitted light profiles. We measure impulse responses of the tensor field with Delta-Pulses as light sources at any (sampled) position and in any direction to generate a uniform sampled map of the global illumination distributions. This map is considered as a global illumination energy flow field. We gain inspiration by vector field particle tracing's FTLE approach for analyzing the gradient of the flow field of the resulting light distributions. Similar to how the FTLE detects ridges/LCS (Lagrangian Coherent Structures) in vector fields (flow fields), our approach captures these structures likewise, attracting/repelling/saddling tensor field lines (TFL) which frequently represent key structures in nature, in tensor fields. We denote this entity a global illumination gradient which states an FTLE-related approach for visualizing LCS in tensor fields through analysis of the global and light transport directed by imprint/engraving in crystelline fiber structures. We also introduce Deformation Ellipsoid Glyphs which are, additionally to visualizing anisotropic topology, pointing inward/outward for compressive/tensile stresses visualizing orientation of principal mechanical stresses. We evaluate our approaches for plausibility and comparability within an extensive test campaign.

Contents

1 Introduction

In this work, we wil discuss the advantages of tensor field analysis and develop a new method for tensor field visualization. At first, we will shortly state the problem setting objectives and then give a quick overview about the structure of this work.

Dieses Kapitel gibt einen Überblick über die Arbeit. Gerade der Abschnitt zur Motivation soll allgemein verständlich geschrieben werden. Die Einleitung sollte auch wichtige Referenzen enthalten.

1.1 Motivation

Tensor Field Visualization is gaining importance as a relevant tool for the analysis of fluid and solid mechanics. Tensors are found most commonly in medical, scientific and engineering applications. A tensor is a n-D generalization of a matrix and appears e.g. as Jacobi-Matrix in Flow Fields or as stress tensor in solid continuum mechanics. Basically, tensors describe stretchings, rotations and volume changes in both solid and fluid material. While most techniques focus on symmetric tensor field visualization (like Glyphs and Tensor Field Lines), some other recent works adress the problem of asymmetric tensor field visualization. The issue with asymmetric or antisymmetric tensors is that they do not always yield real eigenvalues, which is needed to determine an eigenbasis to set up glyphs, hyperstreamlines or tensor field lines. [Zheng and Pang, 2005] et.al. proposed the concept of dual eigenvectors and [Lin et al., 2012] extended it to pseudo-eigenvectors and introduced eigenvector and eigenvalue manifold to visualize eigenvectors in the complex domain.

Worum geht es? Beispiel(e)! Illustrationen sind hier meist sinnvoll zum Verständnis. Warum ist das Thema wichtig? In welchem Kontext?

1.2 Objectives

The problem setting encomprises the visualization of tensor fields, i.e. mostly 2D/3D-grids consisting of mainly second-order tensors (cnf. Cauchy-Stress Tensor). The main

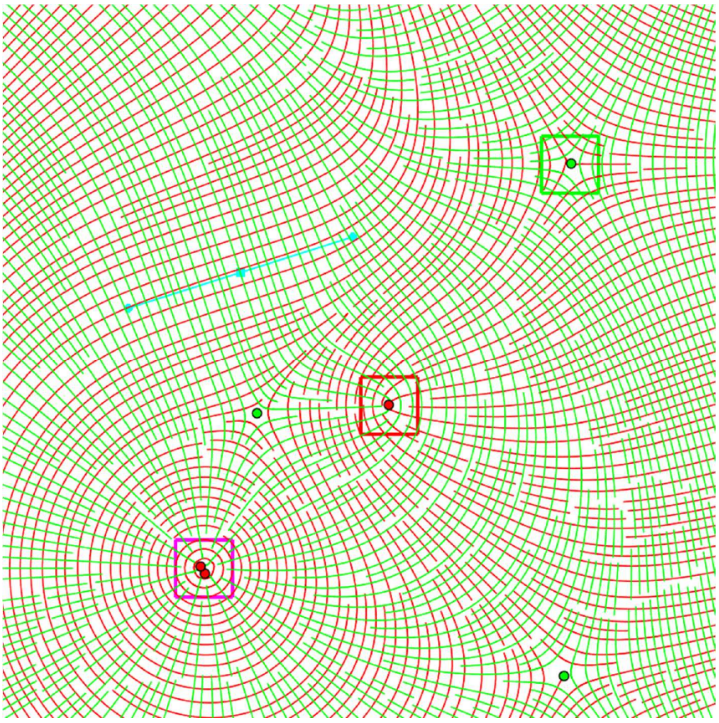

Figure 1.1: Hyperstreamlines in Tensor Field Visualization

purpose of visualization in general is to reduce or encode some set of numbers in some readable, explorable and more intuitive representation. This implies e.g. clustering, structuring or projection techniques. The objective of this work is to develop a simple light propagation scheme to generate a tensor-induced flow map. The tensors are decomposed via singular value decomposition to obtain a real eigenbasis as transmission profile. Another aim is to implement a vector-field visualization borrowed FTLE-related approach in tensor field visualization (both symmetric and asymmetric) for detecting ridges/LCS (Lagrangian Coherent Structures). These structures can be identified as repelling, attracting and saddling (forming a saddle) local features, which frequently represent key structures in nature. LCS usually separate regions of different flow behavior, but in our case they separate regions/domains of differing stress distributions. The map responds most where tensor field lines / hyperstreamlines converge or diverge, whereas one is the same as the other because of bidirectional stress directions. The real part of the eigenvalues can be exploited for sign change (contractions/tensions) which leads to the concept of deformation glyphs w. attached arrows pointing inward/outward for the two types of normal stresses. Practically, in its eigenbasis there are no shear stresses existent for the symmetric stress tensor in equilibrium, just the principal normal stresses. Thus, we can even define the full set of stresses with the deformation glyphs which are derived from the singular value decomposition and signed with the real part of the eigenvalues (in corresponding absolute order).

In diesem Abschnitt sollen neben den Herausforderungen und der Problemstellung insbesondere die Ziele der Arbeit beschrieben werden.

1.3 Structure of this work

For the rest of this work, we will give a quick overview about the structure and outline. Next, in chap. 2, we will capture important fundamentals like Tensors and PCA in the context of singular value decomposition. Also we will discuss the most relevant work in the domain of tensor field visualization. In chap. 3 we will propose the main contribution of this work and document the experimental evaluation in chap. 4. The Summary, Conclusion and Outlook will be given in chap. 5.

Dieser Abschnitt wird meist recht kurz gehalten und beschreibt im Prinzip nur den Aufbau des Rests der Arbeit. Zum Beispiel: In Kapitel 2 geben wir einen Überblick über die Grundlagen zu der Arbeit sowie über verwandte Arbeiten. In Kapitel 3 stellen wir dann …vor. …etc.

2 Fundamentals and Recent Work

In this chapter, we will capture the prerequisites necessary to understand the contributions of this work and will capture Tensors, PCA and Related Work in that sense.

Die ersten paar Abschnitte in diesem Kapitel führen in die Grundlagen zur Arbeit ein. Das können beispielsweise Grundlagen zu Netzwerken oder zur Informationsextraktion sein.

2.1 Tensors

Now what is a Tensor? A tensor is a o-dimensional generalization of a matrix as follows:

order	0	1	2	3	...	o
shape	scalar	vector	matrix	3D-matrix	...	oD-matrix

Table 1: Tensor Shapes

In addition to that, a tensor has as many indices as its order o and their run length is as long as its embedded dimension n, which is equal to the rank of the tensor for full rank. Tensors follow certain transformation rules which are defined for covariant/contravariant tensors. They are most commonly obtained and defined from physical transformation equations. Hence, any oD number array could be a tensor, but the definition holds only if the transformation rules apply to these oD number arrays (in a sense of physical interpretation), which is mostly true for component-indexed oD number entities following matrix multiplication and transformation rules found in physics and math. In fact, tensors themselves are interpreted as a transformation which reflects an incoming direction vector (measuring e.g. the stress in that direction) to an outgoing stress vector. To be a bit more concrete, tensors represent stress distributions in solids and fluids describing strain and flow features as these entities aren't simple numbers or vectors. These numbers just come up as entities or quantities in physics. That is, at each point in space (the grid) there is a whole distribution of e.g. stresses (elastic and viscous) which needs to be characterized and represented.
Cauchy stress tensor

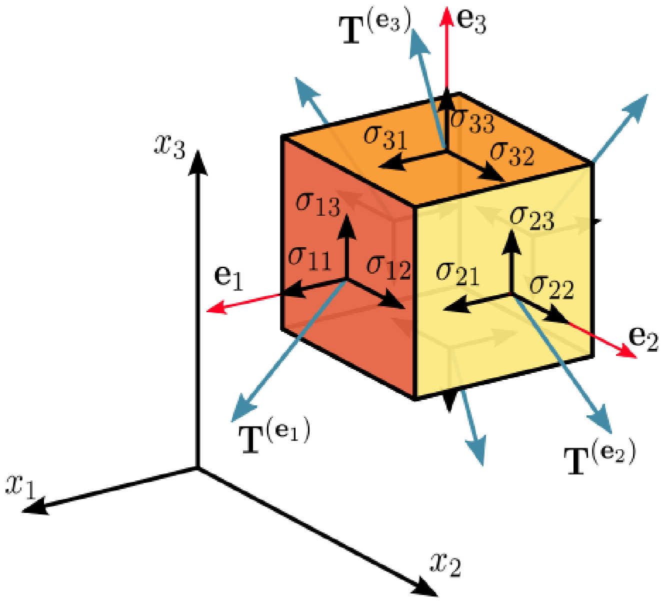

Figure 2.1: Cauchy-Stress Tensor

The Cauchy stress tensor, which is propably the classical example of a tensor, is depicted in Fig. 2.1 and consists of 3 stress vectors $\mathbf{T}(\mathbf{e_i})$ arranged in row-major order. It appears in similar form as viscous stress tensor in fluid mechanics:

$$\boldsymbol{\sigma} = \begin{bmatrix} \sigma_{11} & \sigma_{12} & \sigma_{13} \\ \sigma_{21} & \sigma_{22} & \sigma_{23} \\ \sigma_{31} & \sigma_{32} & \sigma_{33} \end{bmatrix}$$

These 3 stress vectors represent the orientation and magnitude of total resulting stress at plane x, y, z in direction x, y, z (9 individual numbers). Thus, the stress tensor poses a full valid represenation of the stress distribution at any point in space. The stress tensor itself can be interpreted as a transformation which maps an incoming normal direction vector $\mathbf{n}$ a resulting stress vector $\mathbf{T}(\mathbf{n}) = \mathbf{n} \cdot \boldsymbol{\sigma}$. The stresses in normal directions (diagonal elements) are directly related to the pressure, which is always isotropic and hence non-directionally dependent. It is possible to find 3 principal stress directions in 3D, for which there are no shear stresses existent in equilibrium, by PCA (see sect. 2.2 below). These form the principal directions of deformation at a certain location and are sufficient to describe the resulting transformation/deformation behaviour. The resulting system of principal directions and absolute stresses is often called an eigensystem or eigenframe. So to say, an eigensystem consjstent of the principal directions/axes spans a principal ellipsoid depicted in Fig. 2.2 in sect. 2.2.

2.2 Principal Component Analysis

Note that we denote a matrix as a second order tensor interchangeably for the sake of simplicity in the following. For any state of stress in equilibrium it is possible to find n (dimensionality) independent orthogonal directions with no shear stresses existent. Along these directions the principal stresses, which are normal (tensile/compressive) stresses, are exerted. The anisotropy can be represented by ellipsoid glyphs.

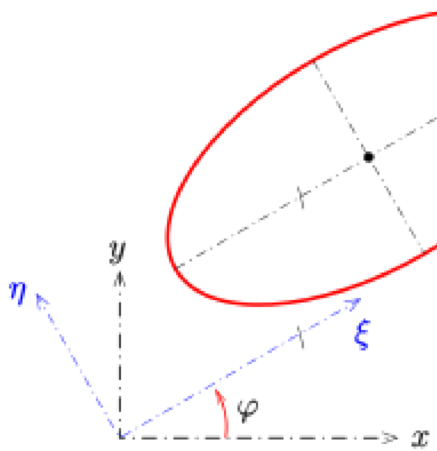

Figure 2.2: Principal Component Analysis

Principal Component Analysis is an algorithm which can capture the principal components (directions) in stochastic data. But it works similarly on transformations to find the principal directions on rotation and scaling. Now, principal component analysis can be done by eigenvalue or singular vector decomposition, whereas the former yields complex eigenvalues for asymmetric matrices. For (anti-)symmetric (normal) matrices, they are connected through the following relation: $s_i = \sqrt{|\lambda_i|}$. Mathematically speaking, a decomposition is somehow decomposing a transformation (which follows certain transformation rules) into parts of subsequent transformations consistent of rotation and scaling ($\mathbf{A} = \mathbf{RSR}^*$). We choose to use singular value decomposition ($\mathbf{A} = \mathbf{U\Sigma V}^*$) to be able to set up real eigenvalues for any kind of matrix (singular values are always real and positive). Also, the singular vectors of the $\mathbf{U}$-matrix represent the half-axes of the principal ellipsoid (eigenframe) shown in Fig. 2.2 for any kind of matrix as suggested by [Moler, 2008]. In addition, we also calculate the eigenvalues to exploit the sign of the real part of the eigenvalues ordered decreasingly by absolute value (corresponding to singular value order). The sign corresponds to tensile (+) and compressive (−) stress, which allows us to visualize deformation glyphs with arrows pointing inwards for compressive and outwards for tensile stresses. We do this decomposition analysis once for each matrix and then store the precomputed results in a grid. The principal ellipsoid is also used as a transmission profile for the propagation scheme in symbolic form in a subequent step.

2.3 Related Work

There has been extensive recent work on symmetric tensors but in comparison little on asymmetric ones. Since we aren't able to cover the whole scope in this work, we will focus on the most relevant works about tensor field visualization.

Symmetric Tensor Field Visualization

[Zheng and Pang, 2005] et.al. proposed a texture-based visualization approach called HyperLIC, which extends the concept of LIC to symmetric tensor fields by using an anisotropic 2D-filter kernel oriented along the major/minor eigenvectors. The notion of tensor field topology and the concept of Hyperstreamlines was first introduced by [Delmarcelle and Hesselink, 1995]. The placement of tensor field lines as hyperstreamlines was recently improved by [Spencer et al., 2009] et.al. for glyph packing. A good overview of seeding strategies is given by [**?**]. [Feng et al., 2008] et. al. used Voronoi Tesselation for placing the glyphs. Superquadric glyphs have been proposed by [Schultz and Kindlmann, for general (non-positive definite) tensors. [de Leeuw and van Wijk, 1993] visualize the partial derivative gradient, the Jacobian of the tensor field to sense the local properties of the field.

Asymmetric Tensor Field Visualization

[Zheng and Pang, 2005] et.al. proposed the concept of dual eigenvectors and [Lin et al., 2012] extended it to pseudo-eigenvectors and introduced the eigenvector/eigenvalue manifolds to visualize eigenvectors in the complex domain. [Palke et al., 2011] et.al. focused on the efficient implementation and visualization of these structures and provided an interactive visualization system for asymmetric tensors applicable in fluid and solid dynamics. In this work, we will use the singular vectors yielded from singular value decomposition to avoid complex values yielded from eigenvalue decomposition. This will allow us to set up glyphs representing the major/minor axis of the underlying transformation for every kind of (asymmetric/symmetric) tensor. We will then use global-illumination techniques to take it one step further and to generate a flow map, permitting us to compute an FTLE-like field on the tensor fields. The concept of Tensor Magnitude has been introduced by [**?**] for means of physical interpretation. They also proposed an efficient glyph and hyperstreamline hybrid approach, which made dynamic interaction in real-time in 2D tensor fields feasible. [Palacios et al., 2015] extracted isosurfaces of tensor magnitude, mode and isotropy index.

Typischerweise im letzten Abschnitt dieses Kapitels wird dann auf verwandte Arbeiten eingegangen. Entsprechende Arbeiten sind geeignet zu zitieren. Beispiel: Die wurde erstmalig in den Arbeiten von Spitz und Gertz [**?**] gezeigt ... Details dazu werden in dem Buch von Newman zu Netzwerken [**?**] erläutert ....

3 Main Part

This chapter will summarize the main contributions of this work studied and state targeted aims and goals as a first step in sect. **??**. Then we will have a short introduction to the implemented global illumination scheme derived and simplified from an nVidia GI approach in sect. 3.2. Last, we will state the effectively developed Visualization methods GIGradient and Deformation Glyphs proposed as innovatively invented tensor visualization techniques.

3.1 Requirements and Ambitions

Our ambition is to develop a simple and efficient Global Illumination Propagation Scheme able to distribute energy profiles in discrete polar form in 2D/3D-space w.r.t. energy conservation and propagation attenuation principles. We then generate transmission profiles from the eigensystems (principal component frames) of the tensors for each cell in the domain (field). That is, to provide an orientation for a grid of crystal fibre structures (cnf. optical fibres) to redirect the intensities in analogy to the anisotropies of the tensor field within a glyph representation, obtained from Principal Component Analysis. Our approach should be implicitly adaptive to any kind of 2D dataset. Thus, we opt to be compatible to handle any kind of matrix (symm./anti-symm.) and any kind of resolution of the field (full-spectrum). At last, we aim to generate a new FTLE-related method for tensor field visualization by applying a Global Illumination Gradient to the resulting light distributions for every possible position and direction of the light source in the grid generated by stimulation with Delta-Impulses. Thus, our motivation is to segment key locations (LCS/ridges) in the field with tensor field lines (hyperstreamlines) converging/diverging, which is necessarily the same (for bidirectional tensor fields). Our approach should efficiently handle (relatively) large datasets. Knapp zwei Seiten, in dem die Anforderungen, die Zielsetzung und die Methoden überblicksartig beschrieben werden. Hier sollte die Beschreibung "technischer" bzw. "formaler" sein als in der Einleitung, da der Leser nun mit den Grundlagen und verwandten Arbeiten vertraut ist.

3.2 Global Illumination Scheme

Within the scope of this work, we will develop a Global Illumination Scheme designed to efficiently propagate the intensities stored in discrete polar coordinates given as impulses (stimuli) by the user or the config. Polar profiles for different light sources are shown in Fig. 3.1:

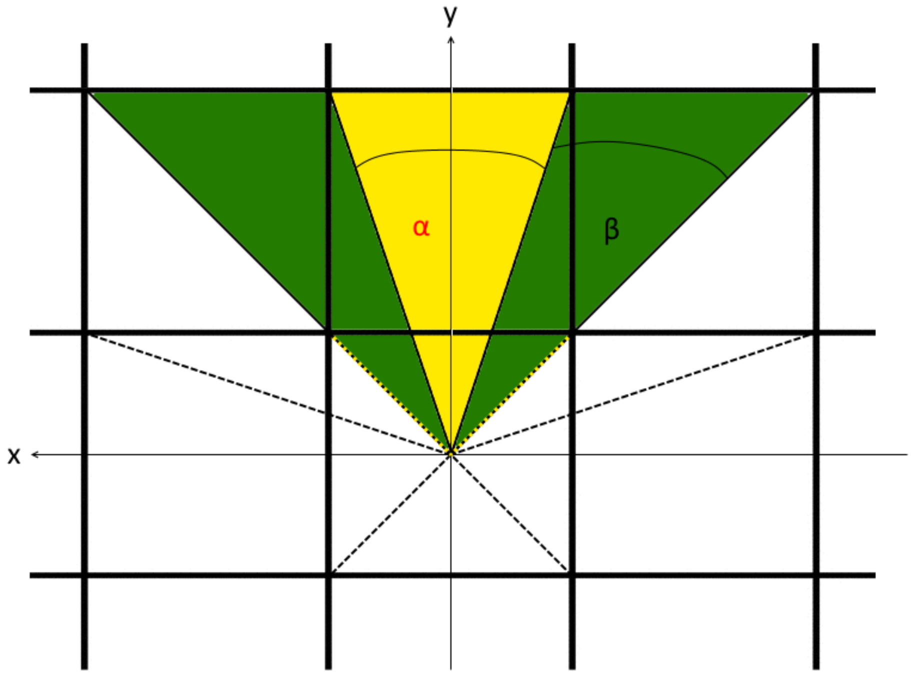

Figure 3.1: Propagation Scheme

Polar profiles map each angle φ a magnitude $\hat{r}$ forming a function $\hat{r}(\varphi)$. They are circular axis versions of the domain $[0..2\pi]$, with negative magnitudes mirrored by 180 degrees). In the sense of interpretability, we exclude negative values (energies) from the scope of our calculations. As a start-up for the propagation, we will think of a grid cell in 2D as a center pixel within an 8-neighborhood. It has 8 (4 faces/edges and 4 diagonals) unique neighbors, which are adjacent point lights in the grid (the type of light source with theoretically no finite extend). We consider one face neighbor (top) to shortly explain the steps of the scheme. The diagonals and the others are obtained from derivation and symmetry.

Each cone (yellow and green) is an individual neighbor-dependent angular area. We optimize for distributing contributions for overlapping cones to transmit attenuated (because of the larger $\sqrt{2}$ distance) intensity in form of a shared part to the diagonals in a single step. Therefore, the intensity gathered in polar coordinates in areas marked in green, need to be partitioned between 2 of the 8 cone-index neighbors as follows:

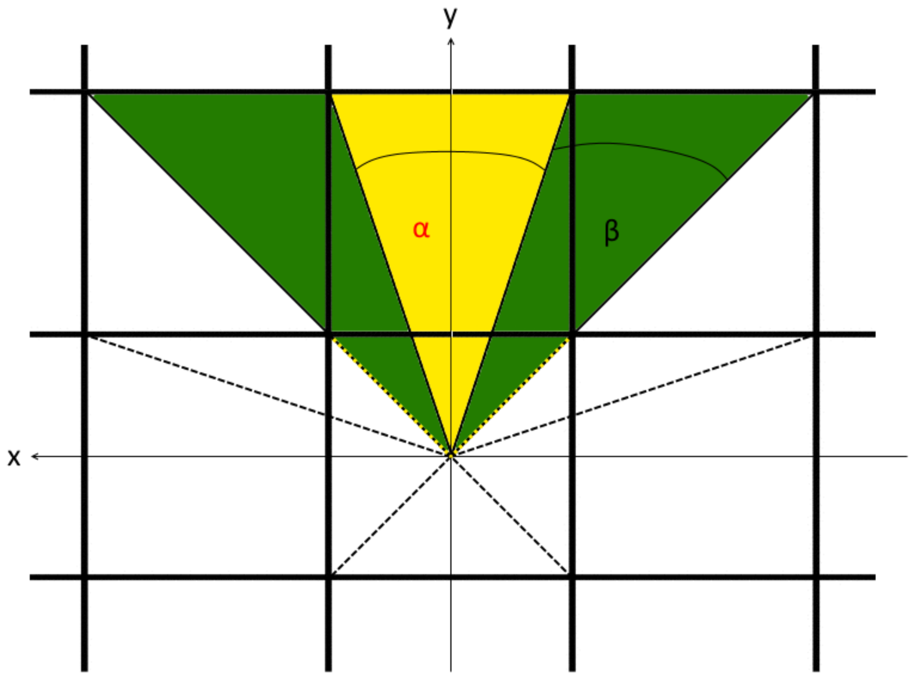

Figure 3.2: Propagation Scheme

The face neighbors take in the angular domain of $d_1 = \alpha + 2\beta$, whereas the diagonal neighbors span a domain of $d_2 = 2\beta$. The linear combination weights for the overlapping (green) parts (β) are obtained from the relative overlapping angular area of β w.r.t. diagonal cones (2β) and face cones ($\alpha + 2\beta = 90°$) (yellow cone is overlapped by green cones at full angle) subsequently normalized to $\sum = 1.0$ (normalization condition):

$$\varepsilon_1 = \frac{\frac{\beta}{\alpha+2\beta}}{\frac{\beta}{\alpha+2\beta} + \frac{\beta}{2\beta}} \approx 0.362291 \tag{3.1}$$

$$\varepsilon_2 = \frac{\frac{\beta}{2\beta}}{\frac{\beta}{\alpha+2\beta} + \frac{\beta}{2\beta}} \approx 0.63771 \tag{3.2}$$

We place a cosine lobe scaled with the integrated energies in each of the 8 cone directions, whereas outgoing integrated and summed energies are weighted by the linear combination weights (factors) in overlapping (green) areas to split up the contributions accordingly. The contribution areas are depicted in Fig. 3.2, the cosine lobes can be observed in Fig. 3.3 respectively. This manner of propagation is inspired by the propagation scheme of [**?**] et.al. (see the paper on how to "project the flux into a point light"). The implementation is done in a dual buffer approach which pushes the energies back and forth (buffer A to buffer B) until convergence, which happens when the energy is spreaded throughout the grid and enters a stationary state, characterized by equal out (at grid borders) to in (at light source positions) energy-flow with no more nettings going on inside the domain. Note that even though we propagate the energy directly through the diagonal cones (which forms a square initially), the 8 degrees of freedom introduce a circular (spherical) wave front after few iterations (for greater resolutions). This occurs, since the diagonals are more strongly attenuated by default and there is a redistribution of intensities in the long term resulting in a circular torus-shaped distribution, as depicted in Fig. 3.3. Also note, that this approach satisfies energy conservation and propagation attenuation principles and applies to the principles of light propagation in vacuum (by default). The verification of these principal requirements and specifications can be observed in the Experimental Evaluation in chap. 4.

We show a few of the first iteration steps for the propagation scheme in Fig. 3.3:

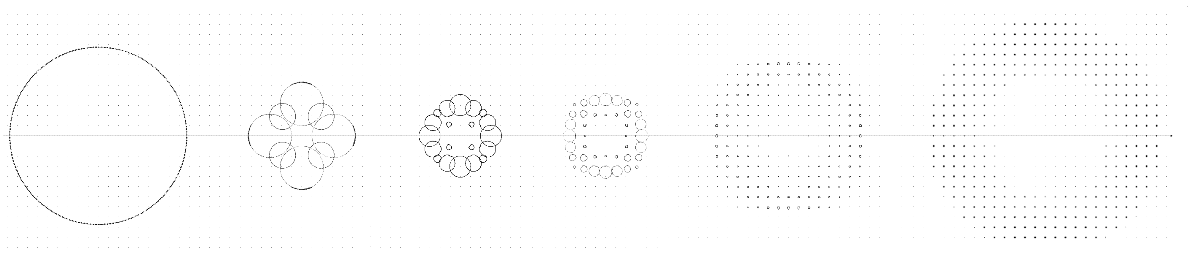

Figure 3.3: Impulse Response for Isotropic Stimulus (Few Iterations: 0,1,2,3,7,11)

It can be proven that the approach follows propagation attenuation principles and follows the inverse (square) law ($\sim \frac{1}{r}$) as observed in the graph in Fig. 3.4.

At last, we define a threshold for the minimum overall distribution error taken into account for convergence conditions, initiating a stop sequence when falling below that threshold. As already mentioned, a dual-buffer approach is chosen here, as we can efficiently propagate from one into the other and just swap pointers to start all over (after reinitialization) and also since it yields a reasonable source-target structure. Until now we aimed to simulate the propagation of light in empty space (vacuum) providing us with a physically-motivated base-approach. We aim to modulate the transmission of the energies on top of the base approach with transmission profiles obtained from the tensor fields through Principal Component Analysis in the following.

In diesem und den nachfolgenden Abschnitten werden die Beiträge der Arbeit motiviert, formal sauber (oft mathematisch, sprich mit Definitionen etc.) beschrieben, und bei Bedarf mithilfe von Beispielen verdeutlicht. Die Beschreibungen in diesem Kapitel sind meist unabhängig von einer konkreten Realisierung und Daten; diese werden im

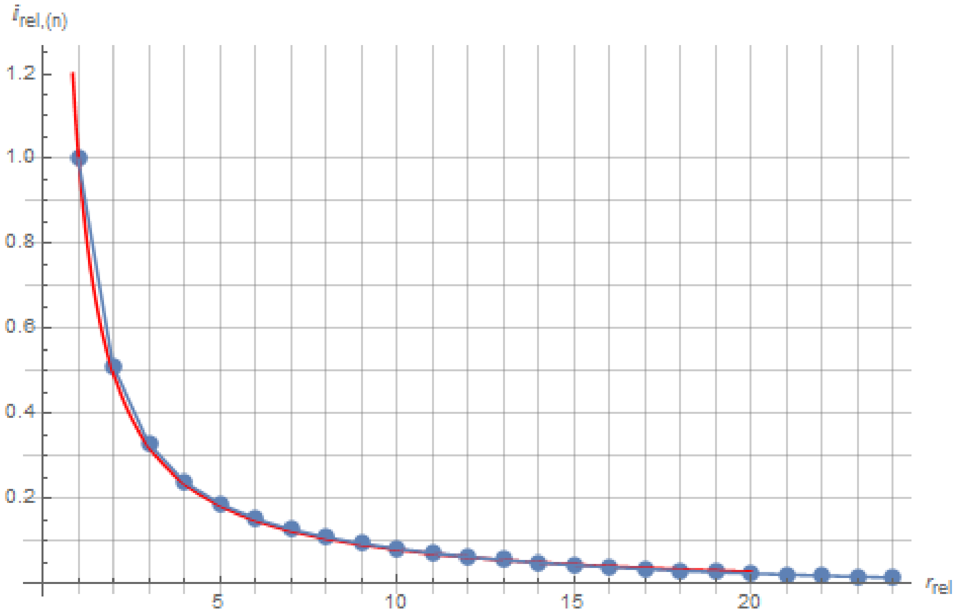

Figure 3.4: Propagation Attenuation

nachfolgenden Kapitel detailliert.

3.3 Transmission Profiles and Weighting

3.4 Global Illumination Gradient

Note that the resulting scalar field is $(n+1)$-dimensional $(x, y, z$ and direction $\theta)$ and needs to be flattened by averaging or projection in 3D for proper visualization. Usw.

4 Experimentelle Evaluation

Der Aufbau dieses Kapitels oder dessen Aufteilung in zwei Kapiteln ist stark von dem Thema und der Bearbeitung des Themas abhängig. Beschrieben werden hier Daten, die für eine Evaluation verwendet wird (Quellen, Beispiele, Statistiken), die Zielsetzung der Evaluation und die verwendeten Maße sowie die Ergebnisse (u.a. mithilfe von Charts, Diagrammen, Abbildungen etc.)

Dieses Kapitel kann auch mit einer Beschreibung der Realisierung eines Systems beginnen (kein Quellcode, maximal Klassendiagramme!).

5 Zusammenfassung und Ausblick

Hier werden noch einmal die wichtigsten Ergebnisse und Erkenntnisse der Arbeit zusammengefasst (nicht einfach eine Wiederholung des Aufbaus der vorherigen Kapitel!), welche neuen Konzepte, Methoden und Werkzeuge Neues entwickelt wurden, welche Probleme nun (effizienter) gelöst werden können, und es wird ein Ausblick auf weiterführende Arbeiten gegeben (z.B. was Sie machen würden, wenn Sie noch 6 Monate mehr Zeit hätten).

Bibliography

[de Leeuw and van Wijk, 1993] de Leeuw, W. C. and van Wijk, J. J. (1993). A probe for local flow field visualization. In *Proceedings Visualization '93*, pages 39–45.

[Delmarcelle and Hesselink, 1995] Delmarcelle, T. and Hesselink, L. (1995). Visualizing second order tensor fields with hyperstreamlines.

[Feng et al., 2008] Feng, L., Hotz, I., Hamann, B., and Joy, K. (2008). Anisotropic noise samples. *IEEE Transactions on Visualization and Computer Graphics*, 14(2):342–354.

[Lin et al., 2012] Lin, Z., Yeh, H., Laramee, R., and Zhang, E. (2012). 2d asymmetric tensor field topology.

[Moler, 2008] Moler, C. (2008). Cleve?s corner: Cleve moler on mathematics and computing. `https://blogs.mathworks.com/cleve/2016/08/08/bug-report-revives-interest-in-svd-option-of-eigshow/`. [Online; accessed 19-July-2008].

[Palacios et al., 2015] Palacios, J., Yeh, H., Wang, W., Zhang, Y., Laramee, R., Sharma, R., Schultz, T., and Zhang, E. (2015). Feature surfaces in symmetric tensor fields based on eigenvalue manifold. *IEEE transactions on visualization and computer graphics*, 22.

[Palke et al., 2011] Palke, D., Lin, Z., Chen, G., Yeh, H., Vincent, P., Laramee, R., and Zhang, E. (2011). Asymmetric tensor field visualization for surfaces. *IEEE Transactions on Visualization and Computer Graphics*, 17(12):1979–1988.

[Schultz and Kindlmann, 2010] Schultz, T. and Kindlmann, G. L. (2010). Superquadric glyphs for symmetric second-order tensors. *IEEE Transactions on Visualization and Computer Graphics*, 16(6):1595–1604.

[Spencer et al., 2009] Spencer, B., Laramee, R. S., Chen, G., and Zhang, E. (2009). Evenly spaced streamlines for surfaces: An image-based approach. *Comput. Graph. Forum*, 28:1618–1631.

[Zheng and Pang, 2005] Zheng, X. and Pang, A. (2005). 2d asymmetric tensor analysis. pages 3– 10.